

mm-WAVE LINAC DESIGN FOR NEXT GENERATION VHEE CANCER THERAPY SYSTEMS*

E. C. Snively[†], K. Deering, E. A. Nanni
 SLAC National Accelerator Laboratory, Menlo Park, USA

Abstract

Direct electron therapy offers an attractive method for providing the high dose rates necessary for FLASH radiation therapy, a new treatment modality with the potential for enhanced healthy tissue sparing. Direct electron therapy has been limited by the low beam energies, up to 20 MeV, provided by today’s medical linacs, restricting the achievable dose depth to superficial tumors. Very High Energy Electron (VHEE) therapy could reach deep-seated tumors throughout the body. A clinically viable VHEE system must provide electron energies of around 100 MeV in a compact footprint, roughly 1 to 2 meters, with modest power requirements. We investigate the development of mm-wave linacs to provide the necessary beam energies on the sub-meter scale, taking advantage of the favorable scaling of high frequency operation to support gradients well above 100 MeV/m. We discuss the design parameters necessary for high efficiency structures, with shunt impedance on the order of 1 GΩ/m, producing high gradients with only a few megawatts of power. We present simulations of cavity performance in the mm-wave operating regime, with an emphasis on compatibility with the requirements of VHEE therapy.

INTRODUCTION

Cancer treatment planning studies have shown that very high energy electron (VHEE) radiation therapy could provide a significant benefit to dose conformity compared to conventional X-ray techniques, allowing doctors to treat previously incurable cancers because of the improved sparing of healthy tissue [1]. VHEE is also a promising candidate for improving cancer treatment through FLASH therapy [2]. Because VHEE uses the accelerated beam of electrons directly, the high dose rate required for FLASH treatments can be achieved about 20 times more efficiently than with X-rays. The significant charge required for the FLASH dose rate, on the order of 160 nC corresponding to a cumulative 16 J of energy for 100 MeV electrons delivered in a fraction of a second, necessitates that the acceleration be achieved with an RF-driven process rather than alternative compact techniques like laser-plasma and laser-structure based acceleration.

To develop structures with the ≥ 100 MeV/m accelerating gradients needed for compact VHEE, a key design strategy will be operation at higher frequencies than conventional linacs, because the threshold voltage for plasma breakdown, which limits the achievable gradient, has been

shown empirically to scale as the square root of the driving frequency in accelerating structures. Linacs operating in the mm-wave regime may provide a technological solution to the unmet need for VHEE accelerators, with the capacity to reach well above 100 MeV in a clinically compatible footprint of less than a meter. Comparison of the shunt impedance and structure size needed to achieve a 100 MeV beam with 20 MW of power, for the case of a mm-wave linac and an X-band linac, a more conventional, but still high frequency operating regime. The efficiency of the acceleration is characterized by the shunt impedance, R_s , defined in terms of the accelerating voltage per meter, V_s , and dissipated power per meter, P_{disp} , as $R_s = V_s^2/P_{disp}$. The parameters shown in Table 1 use the best shunt impedance demonstrated at SLAC for X-band [3] and mm-wave [4-6] structures and extrapolate based on expected enhancement at cryogenic temperatures.

In general, the limiting factor on advances in mm-wave technology has been the availability of high power sources. However, a high efficiency mm-wave structure could provide VHEE beams in a footprint significantly shorter than a meter using input powers well within the range accessible with today’s gyrotron technology [7], if active pulse compression can be utilized [8, 9].

Table 1: Cryogenic Linac Comparison for VHEE

Name	X-band linac	mm-wave linac
Frequency	11.424 GHz	100 GHz
Shunt impedance, R_s	430 MΩ/m	1 GΩ/m
Structure length	1.16 m	0.5 m
Beam energy, given 20 MW input power	100 MeV	100 MeV

Commercially available sources have the efficiency and total average power needed to drive our structures, but pulse compression techniques will be critical for achieving the peak powers and pulse shaping required to match the pulse format for driving the accelerating structure. Here, we investigate the design of a linac operating at 94 GHz that will provide beam energies up to 10 MeV in a few centimeters, a sufficient range for superficial tumor treatment and pre-clinical animal studies of the FLASH effect.

LINAC DESIGN OVERVIEW

We consider the case of a standing wave cavity with 180° phase advance per cell. The re-entrant nose cone of the cavity geometry is tailored to maximize the shunt impedance and significantly reduces the coupling between cells. A model of the first 12 cells of the linac structure is

* Work supported by U.S. Department of Energy Contract No. DE-AC02-76SF00515, SLAC LDRD project 21-014 and Internal Agency Agreement 21-0007-IA (MIPR HR0011150657).

[†] esnively@slac.stanford.edu

shown in Fig. 1. The length of each subsequent cell is increased in this initial section in order to compensate for the increase in beam velocity from non-relativistic to relativistic. The specific topology of each individual cell has been optimized for maximum acceleration, at the resonant frequency of 94 GHz.

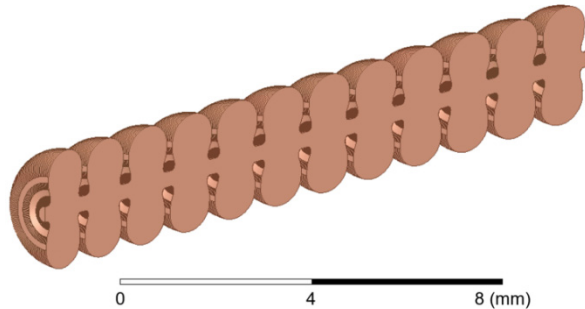


Figure 1: Vacuum space of one half of a 12 cell standing wave linac geometry modelled in HFSS with tapered cell length to accommodate acceleration from nonrelativistic to relativistic electron energies.

At just 100 kW per cell operating at room temperature, this 12 cell section brings a nonrelativistic electron bunch of a few hundred keV up to over 3 MeV. The on-axis field enhancement within the cell produced by the re-entrant nose cones is clear in the cross-sectional plot of the electric field shown in Fig. 2, while the field is drastically reduced in the beam pipe between cells. The peak shunt impedance, reached in the 12th cell, is 438 MΩ/m at room temperature. Design parameters for this cell are given in Table 2. We plan to operate our structure at cryogenic temperatures and expect an improvement to the shunt impedance by at least a factor of 2 when operating at liquid nitrogen temperatures of 77 K, putting us in range of our goal of 1 GΩ/m shunt impedance. Beyond the initial section that spans non-relativistic beam energies, cell-by-cell optimization will become less critical as the beam has already reached a

relativistic velocity. We explored extending our linac structure with additional cells, identical in topology to the 12th cell design, in order to reach our target beam energy of 10 MeV. We discuss beam dynamics simulations using General Particle Tracer (GPT) below.

Table 2: Linac Design Parameters

Name	Unit	Prototype
Frequency, f	GHz	94
Iris Aperture Radius, a	μm	170
Iris Thickness, t	μm	200
Quality Factor, Q_0		3295
Power per cell, $P_{\text{dissipated}}$	kW	100
Accelerating Gradient, E_{acc}	MeV/m	167
Max. Surface Elec. Field, E_{max}	MV/m	430
Max. Surface Mag. Field, H_{max}	kA/m	417
$E_{\text{max}}/E_{\text{acc-periodic}}$		2.57

BEAM DYNAMICS SIMULATIONS

Results from a simulation study using the cavity design presented above are shown in Fig. 3 with the simulated input parameters shown in Table 3. As predicted by our HFSS model of fields in the structure, we see an energy gain of 3 MeV over the first 12 cells, and full acceleration up to 10 MeV with an extended 38 cell structure, given an input power of 100 kW per cell operating at room temperature. GPT simulations comparing different total beam charge, with space charge effects included, show an increase in normalized radial rms emittance of 5 nm·rad for 50 fC and 100 fC, and up to 25 nm·rad for the case of a 1 pC beam. This result is a promising indication that we will be able to scale the performance of our structure to the charges we need for FLASH therapy dose rates.

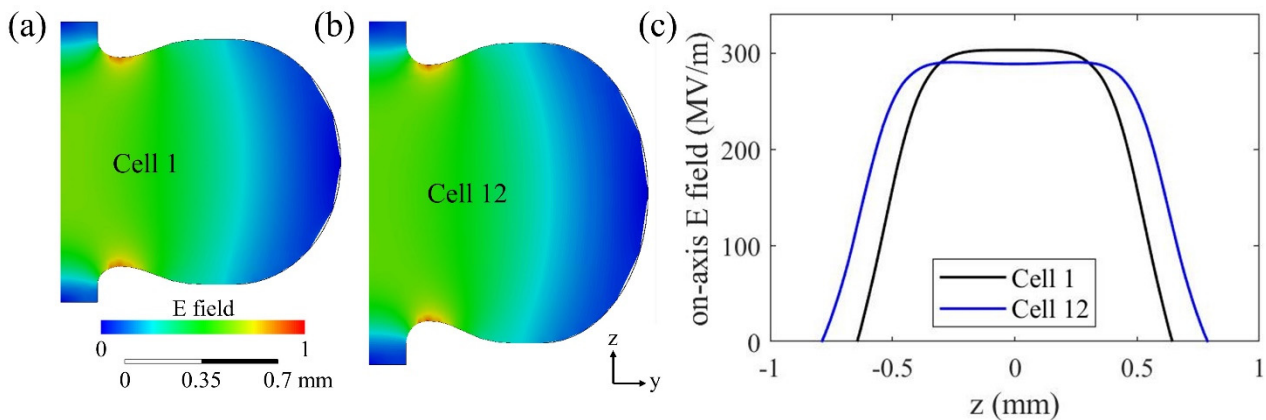


Figure 2: Normalized electric field distribution for the π -mode in half of the cell cross-section for (a) the 1st cell, with the shortest length corresponding to lowest beam energy, and (b) the 12th cell, beginning the 27-cell section with fixed cell period. The beam propagates along the z -axis. (c) The electric field along the z -axis for 100 kW input at room temperature.

For a proof-of-principle test of this linac, we plan to operate our prototype with a 50-100 fC beam. Our predictions for the input beam are based on simulations of SLAC's THz field emission gun designed by S. M. Lewis *et al.* for operation at 110 GHz [10]. We have already reproduced simulations of this field emission gun in GPT and integrated the input deck with our linac model in order to simulate full start-to-end beam dynamics. As we proceed with our design work, we will investigate rescaling this THz gun for operation at our intended frequency of 94 GHz.

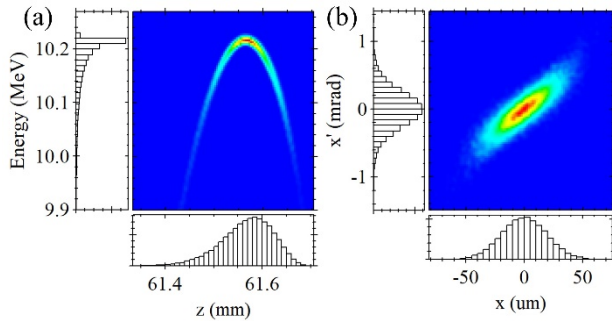


Figure 3: (a) Longitudinal and (b) transverse phase space of a 100 fC beam at the exit of the 38 cell linac operating at 94 GHz with 100 kW per cell at room temperature.

Table 3: Simulated Initial Beam Parameters

Name	Unit	Prototype
Charge	fC	100
Initial Beam Energy	keV	347
RMS spot size	μm	20
Bunch length, σ	μm	30
Normalized radial emittance	nm-rad	50
Divergence	mrad	0

PROTOTYPE DESIGN

In addition to the cell geometry, we are investigating several coupling configurations as well as different methods of tuning the cells. These design elements will be critical to the successful operation of the structure. Because we have optimized the cell geometry for maximum shunt impedance using re-entrant nose cones, we have selected a distributed coupling technique that does not rely on any coupling between cells. This design has precedent with the W-band power extractor designed by F. Toufexis *et al.* for SLAC's RF undulator concept operating at 91 GHz [4]. In their design, the power extracted from a high energy electron beam passing through 40 cavities is coupled out to a manifold that combines that power to provide a source for the RF undulator. While our application is different, the principles of the distributed coupling will remain the same. Our prototype will also incorporate a field emission gun, modelled after the copper tip and 2 cell design developed

by S. M. Lewis, *et al.* [10]. We anticipate using a split-block configuration for the mechanical design of the linac and coupling manifold.

CONCLUSION

In addition to the prototype design and fabricating process, we will continue start to end simulations of this mm-wave structure using GPT. The planned simulation study will look at the system performance given an initial beam produced through field emission, from both the intended copper tip and dark current from the walls of the cavity due to the high fields in the structure. We will also extend our structure model to be able to reach beam energies up to 100 MeV. Ultimately, this full structure simulation will produce beam phase space data to be used in dose deposition studies for direct electron therapy.

While extensive simulation studies have been done on VHEE therapy, there is currently no clinically compatible system in existence that can provide the electron energies required. Our research to develop a VHEE accelerator in the mm-wave regime must overcome the constraints on available in put power. While the proposed system can still leverage commercial RF sources, it will require new pulse compression techniques, without the support of an extensive body of existing research or clinical infrastructure. However, as truly novel technology, mm-wave structures offer the potential for a more transformative leap in terms of the compactness and accessibility of medical accelerators, as well as an extended range of beam energies that can be achieved within a clinically compatible system.

ACKNOWLEDGEMENTS

The authors thank Billy Loo, Sami Tantawi, Samantha Lewis, Mohamed Othman, Matthew Franzi, Sam Schaub, Brad Hoff, and Julian Merrick for helpful discussions.

REFERENCES

- [1] M. Bazalova-Carter *et al.*, "Treatment planning for radiotherapy with very high-energy electron beams and comparison of VHEE and VMAT plans", *Medical Physics*, vol. 42, no. 5, pp. 2615–2625, Apr. 2015.
doi:10.1118/1.4918923
- [2] M. -C. Vozenin *et al.*, "The Advantage of FLASH Radiotherapy Confirmed in Mini-pig and Cat-cancer Patients", *Clinical Cancer Research*, vol. 25, no. 1, pp. 35–42, Jun. 2018. doi:10.1158/1078-0432.ccr-17-3375
- [3] S. Tantawi *et al.*, Distributed Coupling Accelerator Structures: A New Paradigm for High Gradient Linacs, 2018, arXiv:1811.09925
- [4] F. Toufexis *et al.*, "Development of a W-Band Power Extraction Structure", SLAC National Accelerator Lab., Menlo Park, CA, United States, Rep. THPTS063, Jun. 2019. doi:10.18429/JACoW-IPAC2019-THPTS063
- [5] E. A. Nanni *et al.*, "Results from mm-Wave Accelerating Structure High-Gradient Tests", in *2018 43rd International Conference on Infrared, Millimeter, and Terahertz Waves (IRMMW-THz)*, Nagoya, Japan: IEEE, 2018, pp.197-199.
doi:10.1109/irmmw-thz.2018.8510478

- [6] M. A. K. Othman *et al.*, “Experimental demonstration of externally driven millimeter-wave particle accelerator structure”, *Applied Physics Letters*, vol. 117, no. 7, p. 073502, Aug. 2020. doi:10.1063/5.0011397
- [7] M. Thumm, “State-of-the-Art of High Power Gyro-Devices and Free Electron Masers. Update 2016”, KIT Scientific Publishing, Karlsruhe, Germany, Rep. KIT-SR 7735, Jul. 2017. <https://publikationen.bibliothek.kit.edu/1000068193/4234530>
- [8] S. G. Tantawi, R. D. Ruth, A. E. Vlieks, and M. Zolotarev, “Active high-power RF pulse compression using optically switched resonant delay lines”, *IEEE Transactions on Microwave Theory and Techniques*, vol. 45, no. 8, pp. 1486–1492, Aug. 1997. doi:10.1109/22.618460
- [9] S. V. Kutsaev *et al.*, “Nanosecond rf-Power Switch for Gyrotron-Driven Millimeter-Wave Accelerators”, *Physical Review Applied*, vol. 11, p. 034052, Mar. 2019. doi:10.1103/physrevapplied.11.034052
- [10] S. M. Lewis *et al.*, “Design of a High Gradient THz-Driven Electron Gun”, SLAC National Accelerator Lab., Menlo Park, CA, United States, Rep. TUPTS077, Jun. 2019.